Published in Surface Science 417, issue 1, 41-52, 1998
which should be used for any reference to this work

Photoelectron emission from nitrogen- and boron-doped diamond (100) surfaces

L. Diederich *, O.M. Küttel, P. Ruffieux, Th. Pillo, P. Aebi, L. Schlapbach

Physics Department, University of Fribourg, Pérolles, 1700 Fribourg, Switzerland

Abstract

The nitrogen-doped (N-doped), type Ib, synthetic diamond (100) surface was investigated by means of X-ray photoelectron spectroscopy (XPS) and ultraviolet photoelectron spectroscopy (UPS). Photoelectron emission data from the boron-doped (B-doped) and the N-doped diamond (100) surfaces were compared and permitted the energy band diagrams for these differently terminated surfaces to be drawn. We observed emission from energy levels below the conduction band minimum up to the vacuum level and therefore succeed in evaluating the negative electron affinity (NEA) of the hydrogen-terminated diamond surfaces. Both the hydrogen-terminated N- and B-doped diamond (100) surfaces show NEA values of at least -0.2 and -1.0 eV, respectively, while the hydrogen-free surfaces show positive electron affinity. In contrast to the hydrogen-terminated B-doped (100) surface, UPS measurements on the hydrogen-terminated N-doped (100) surface do not reveal a high intensity NEA peak owing to the strong upward band bending. The high intensity NEA peak of B-doped diamond seems to be due to the downward band bending together with the reduced work function because of hydrogen termination. The work function increases for subsequent hydrogen desorption at higher annealing temperatures with associated loss of NEA. For the N-doped diamond (100) surface the work function behaves similarly but the observation of a NEA peak is absent because of the surface barrier formed by the upward band bending.

Keywords: Diamond; Hydrogen; Low index single crystal surfaces; Photoelectron spectroscopy; Surface structure

1. Introduction

Important progress in chemical vapor deposition [1–3] (CVD) of diamond in order to produce (100) and (111) oriented, textured, and boron-doped (B-doped) films together with the negative electron affinity (NEA) characteristic of these surfaces has stimulated interest to develop NEA diamond-based electronic devices for high-frequency, high-temperature and high-power applications. Doping diamond with electronically active impurities (n- and p-type) is necessary for many of these semiconductor device applications. With the exception of boron, all impurity atoms are larger and will deform the diamond lattice because of the small tetrahedral radius of carbon (0.77 Å). Boron and nitrogen are the only impurities in diamond, which have been shown to be *substitutional* [3]. In most natural diamonds (type Ia diamond) nitrogen, in fairly substantial amounts, is present as aggregate or is located on *interstitial* positions in the crystal lattice. Synthetic, high-pressure, and high-temperature diamonds, which are yellowish in color contain nitrogen on *substitutional* sites and are called

* Corresponding author. Present address: University of Milan, INFM Department of Physics, via Celoria 16, I-20133 Milan, Italy. Fax: +39 2 239 24 87; e-mail: diederich@mi.infn.it

type Ib diamonds. Measurements of photoconduction, optical absorption, and resistance as a function of temperature in type Ib diamonds suggest that the level due to substitutional nitrogen is situated 1.7 eV below the conduction band minimum (CBM) [4,5]. Because nitrogen forms a deep donor level in diamond, it is electrically inactive at room temperature as a dopant but plays an important role in the recombination and compensation of electrical carriers. Very few diamonds are effectively free of nitrogen (type IIa diamond) and have enhanced optical and thermal properties owing to their strongly insulating behavior. The type IIb diamond is a pure (free of nitrogen) and type of diamond rare in nature, which shows p-type semiconducting properties. This semiconducting behavior is due to substitutional boron acceptors in diamond at 0.36 eV [1] above the valence band maximum (VBM). Boron is the only impurity that has been successfully doped into diamond to fabricate thin p-type CVD films for device applications. No shallow n-type dopants have been found, although n-type behavior of diamond doped with nitrogen, phosphorus, sodium and lithium has been reported or predicted [1]. As a matter of fact, in most cases, the n-type behavior was associated with defects created during the introduction of the impurities (ion implantation) because the semiconducting properties could not be sustained following high temperature annealing. However, CVD investigations have shown that small quantities of nitrogen added in the gas phase during the CVD of diamond lead to beneficial changes in the growth rate, texture and morphology [6,7].

Very recently Okano et al. [8] reported heavily nitrogen-doped (10^{20} cm^{-3}) diamond films grown by CVD which show field emission of electrons at a threshold voltage less than 0.5 V μm^{-1} which augurs well for cold cathode technology. The nitrogen-doped (N-doped), type Ib, synthetic diamond has received much interest since Geis et al. [9] reported field emission of electrons from N-doped diamond. Emission from B-doped diamond requires vacuum electric fields of 20–50 V μm^{-1} [9]. Their measurements showed that N-doped diamond requires fields of only 0–1 V μm^{-1}. In order to explain this behavior an NEA of -0.7 eV was assumed for this type of diamond and -1.7 eV for the O–Cs-treated diamond [10] for the emission of electrons into vacuum. Recently, the same group presented a cold cathode emitter based on a field emission Spindt cathode using a diamond film doped by substitutional nitrogen [11]. The device shows high field emission currents with a low voltage of 0–1 V μm^{-1}. Such a Geis–Spindt diamond field emitter has been studied theoretically [12]. The cathode performance is limited by the injection of electrons into diamond from the back-metal contact while the emission performance is explained by the stable NEA of diamond, which allows the injected electrons in the diamond to be emitted into vacuum with low electric fields of 0–1 V μm^{-1}.

Natural, B-doped diamond surfaces have been investigated using various experimental techniques, such as Auger electron spectroscopy [13], ion scattering [14], thermal desorption [15], high-resolution electron energy-loss spectroscopy (HREELS) [16], X-ray and angle-resolved ultraviolet photoelectron spectroscopy (XPS, ARUPS) [13,17–19], and X-ray photoelectron diffraction (XPD) [20]. These surface-sensitive techniques require a very low surface roughness and no surface contamination. Our natural diamond surfaces were cleaned by a microwave hydrogen plasma at 870°C and at a pressure of 40 mbar [21]. Low energy electron diffraction (LEED) patterns [18] and scanning tunneling microscopy (STM) images [22] of the B-doped (100) surface confirm the (2×1) reconstruction which is stable even in air. STM images show large, atomically flat terraces for the B-doped hydrogen plasma treated (100) surface, which is an indication of the efficient surface polishing. The hydrogen-terminated (2×1) reconstructed (100) surface ((100)-(2×1):H surface) prepared in this way is assumed to have a monohydride surface termination [15,16], also confirmed by calculations [23–25]. It shows NEA behavior, experimentally observed using UPS [18] and calculated using ab initio molecular dynamics [26]. Annealing the crystal to 1100°C in ultrahigh vacuum results in a hydrogen-free (2×1) reconstructed (100) surface ((100)-(2×1) surface) where the π-bonded dimers are responsible for the forma-

tion of surface states [19]. This surface termination shows positive electron affinity (PEA) [18,23,26].

The N-doped, type Ib diamond is a potential material for cold-cathode field emitters characterized by high field emission currents at very low power [8,11]. Smentkowski et al. [27] presented XPS measurements from the N-doped diamond (100) surface. Annealing the surface to temperatures up to 1200°C resulting in a (100)-(2×1) surface leads to an increasing upward band bending due to the donor ability of the nitrogen as shown by their XPS results. Up to now, UPS measurements from the N-doped, type Ib diamond (100) surface have not been realized and, hence, it is not known whether such diamonds show NEA, too. Calculations show that, for the diamond (100) surface, the vacuum level E_{vac} is thought to be about -2.2 eV [26] (for the (100)-(2×1):H surface) and -0.8 eV [28] (for the cesiated (100) surface) below the CBM. However, an NEA of 2.2 eV for the N-doped diamond (100) surface would result in a work function of -0.5 eV, being a very questionable value.

Here we present UPS measurements from the N-doped, type Ib diamond (100) surface for different annealing temperatures. Photoelectron spectroscopy measurements from the B- and N-doped diamond (100) surfaces are compared with each other. In this article Section 2 describes the experimental setup while Section 3 presents the photoelectron spectroscopy measurements of the N- and B-doped diamond (100) surfaces, respectively. In Section 4 the results are summarized in the energy band diagrams whereas in Section 5 we conclude.

2. Experimental

The diamond (100) substrates used in this study are a Ib (N-doped, $N_D=10^{20}\,cm^{-3}$) 3 mm × 4 mm synthetic crystal (commercial substrate grown using high-pressure techniques [1]) and a IIb (B-doped, $N_A=10^{16}\,cm^{-3}$) 5 mm × 5 mm natural crystal. Both are oriented within 3° of the (100) crystallographic plane. The crystals were mechanically polished by Meyer AG (Biel, Switzerland). The surfaces were cleaned by a microwave hydrogen plasma at 870°C and at a pressure of 40 mbar in order to avoid any surface contamination [29]. After hydrogen plasma cleaning the samples were mounted on a heatable (up to 1200°C) sample holder and transferred at ambient conditions to a VG ESCALAB Mk II spectrometer with a base pressure of 2×10^{-11} mbar, equipped with an Mg Kα ($h\nu=1253.6$ eV) and a Si Kα ($h\nu=1740.0$ eV) twin anode, a helium discharge lamp (He I, $h\nu=21.2$ eV; He II, $h\nu=40.8$ eV) and a LEED system. The energy resolution is at its best 0.9 eV for XPS and 35 meV for UPS (He I). Annealing temperatures of the diamond sample were measured with a two-color pyrometer, which was previously calibrated with a thermocouple.

We annealed the N- and B-doped diamond (100) surfaces to temperatures up to 1100°C at pressures remaining in the 10^{-10} mbar range while the XPS and UPS (only for the B-doped diamond) measurements were performed at room temperature. Since the N-doped diamond (100) surface is insulating at room temperature, the charging effects were compensated by illuminating the crystal by an argon ion laser ($\lambda=514$ nm, $P=25$ mW) for the XPS measurements and by doing the UPS measurements at a substrate temperature of 400°C. The measurements at 400°C were performed in a mode with alternating heating and measuring cycles (50 Hz) to avoid disturbing electric and magnetic fields due to the sample heating current.

3. Results

3.1. Principle of UPS for low kinetic energy electrons

In order to understand better the determination of energy levels in our UP spectra, we show in Fig. 1 combined He I, He II spectra and the corresponding band schemes for the NEA (Fig. 1a) and PEA (Fig. 1b) cases, respectively. For diamond surfaces, the states near E_F are better probed by the He II spectra. The reason for this is the more favorable photoemission cross-sections for He II. The cross-section of the 2p states at 8.0 eV binding energy is lower for a photon energy of 40.8 eV than for an energy of 21.2 eV but it is

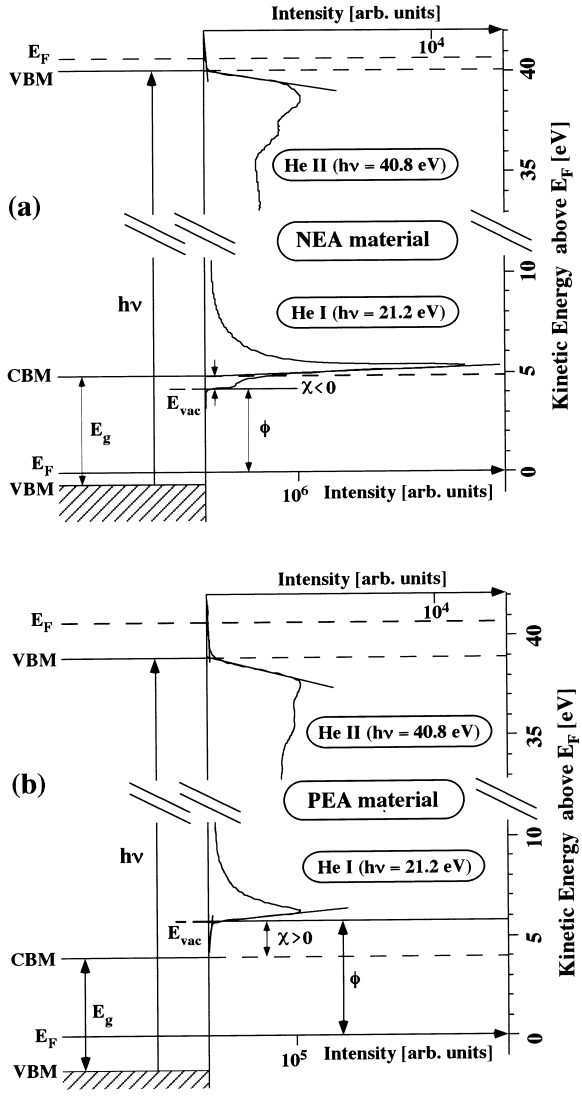

Fig. 1. Combined He I ($h\nu = 21.2$ eV) and He II ($h\nu = 40.8$ eV) normal emission spectra of the valence band for (a) negative electron affinity (NEA) and (b) positive electron affinity (PEA) materials with the band diagrams on the left side, respectively. We determine the energy levels at the cutoff positions with extrapolation to zero intensity. Labeled are the work function ϕ, the electron affinity χ, the band gap E_g, the vacuum level E_{vac}, the photon energy $h\nu$, the Fermi level E_F, the conduction band minimum (CBM), and the valence band maximum (VBM). Note the different intensity scales for the spectra of the (a) NEA and (b) PEA cases.

higher for states near E_F. We determine the VBM position near E_F in the He II parts of the spectra (Fig. 1a and 1b) by extrapolation of the VBM to zero intensity, estimating an error of 0.1 eV. This error value is estimated from the error for the determination of the energy position and by the reproduction of the results (surface preparation). The VBM is extrapolated to zero intensity because the valence band of a semiconductor has a continuously decreasing distribution in contrast to metals where the tailing off is in part due to the spread in the Fermi distribution and therefore the Fermi level is determined at half maximum. We proceed in the same way as Cardona and Ley [30] or Hansson and Uhrberg [31] who have described the determination of the VBM for the silicon (100)-(2×1):H and (100)-(2×1) surfaces. The determination of the VBM position in the He II parts of the spectra is only correct provided that there are no occupied surface states and that states near the Γ-point of the bulk Brillouin zone (BZ) are probed. The diamond (100)-(2×1):H surface is known to have no occupied surface states near E_F [19,32], states near the Γ-point of the bulk BZ are probed (with the photon energy of 40.8 eV we are less than 0.2 Å^{-1} away from the Γ-point at normal emission) and therefore the determination of the VBM for this surface termination is possible.

When a diamond surface shows NEA, electrons thermalizing to the CBM are emitted very easily into the vacuum. They appear in the He I spectra (Fig. 1a) as a sharp high intensity peak at low kinetic energy (around 5.0 eV) and the energy position determines the CBM (because E_{vac} lies below). The relative position of the CBM with respect to E_F is chosen by the cutoff of the NEA peak with extrapolation to zero intensity (Fig. 1a) within an error of 0.1 eV. We use the same arguments for the CBM determination as for the VBM determination [30,31]. The determination of the CBM from the NEA peak permits us to have a fingerprint for the determination of the energy distance VBM$-E_F$. In fact, deducing the energy distance E_F-CBM from the band gap (5.5 eV), we obtain the energy distance VBM$-E_F$ which must be identical to that determined with the He II spectra.

However, depending on the spectrometer used, these low energy electrons cannot overcome the work function of the electron analyzer and hence, cannot be detected. Therefore, a low negative bias

between 0 and -10 V is applied to the sample [18,30]. This applied bias voltage also eliminates the problem of secondary emission from the walls of the sample chamber and other parts of the spectrometer. For an applied bias of -1.5 V or below, the cutoff positions of the spectra do not further change. For PEA the vacuum level lies above the CBM and, therefore, the low energy cutoff in the spectra with extrapolation to zero intensity determines E_{vac} (Fig. 1b). [30,31]

Another important component for the energy band diagrams is the bulk Fermi-level position. It is known that boron forms the acceptor level in the type IIb diamond with an ionization energy of $E_A = 0.36$ eV [1,33,34]. By requiring charge neutrality, Bandis and Pate [35] calculated the bulk Fermi-level position of B-doped diamond as a function of temperature and impurity concentration. For the B-doped ($N_A = 10^{16}$ cm^{-3}) diamond, our analogous calculations predict the bulk Fermi level at 0.30 eV [36] above the VBM in agreement with the calculations of Bandis et al. [35]. The energy distance $E_A - E_F$ in this case is 0.06 eV. The nitrogen forms a deep donor level in the type Ib diamond with an ionization energy of $E_D = 1.7$ eV [4]. For the N-doped ($N_D = 10^{20}$ cm^{-3}) diamond, our calculations predict the bulk Fermi level at 1.6 eV [36] below the CBM, 0.1 eV above the deep donor level (situated 1.7 eV [4] below the CBM).

3.2. Nitrogen-doped synthetic diamond (100) surface

After hydrogen plasma cleaning [21], the N-doped diamond (100) surface presents a (2×1) reconstruction as shown in the LEED pattern ($E = 154.7$ eV) of Fig. 2. The spots corresponding to a bulk termination are marked by white squares while the other spots characterize the two domains of the (2×1) superstructure. The LEED pattern, measured at room temperature, is visible down to 60 eV electron energy. The hydrogen-saturated (100) surface prepared with this technique is assumed to have a monohydride surface termination [15,16,23–25] and is denoted (100)-(2×1):H. It presents no surface contamination as shown by the Mg Kα XP normal emission overview spectrum in Fig. 3. Hence, the microwave hydrogen plasma is well suited to prepare very clean natural diamond surfaces and to obtain reproducible results

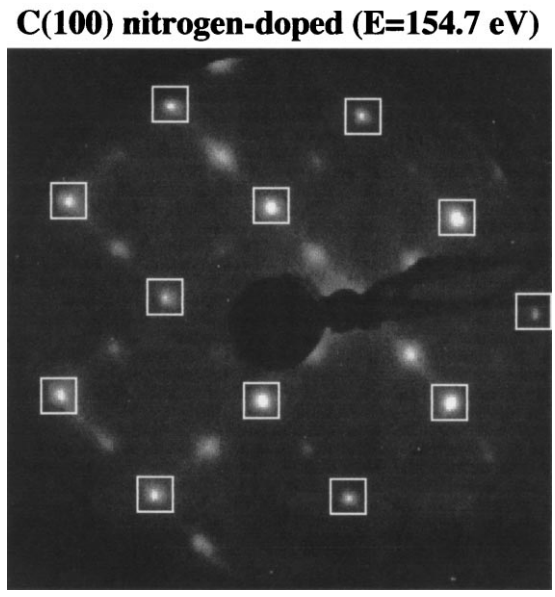

Fig. 2. LEED pattern ($E = 154.7$ eV) from the hydrogen plasma treated N-doped diamond (100) surface which reveals a (2×1) reconstruction. The spots corresponding to a bulk termination are marked by white squares while the other spots characterize the two domains of the (2×1) superstructure.

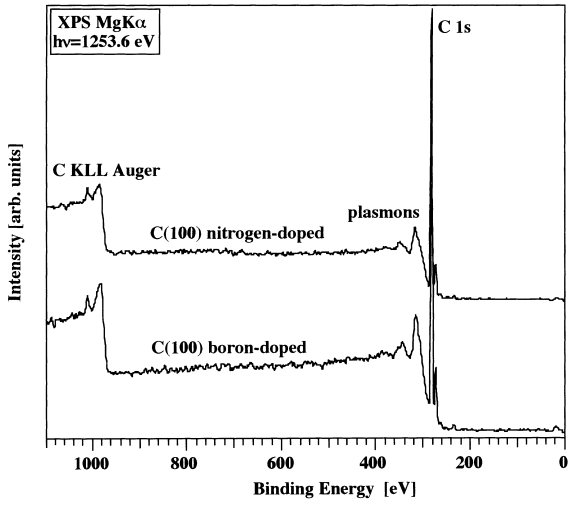

Fig. 3. XP normal emission overview spectra from the hydrogen plasma ($T = 870$°C, $p = 40$ mbar) cleaned B- and N-doped diamond (100) surfaces. The oxygen coverage is less than 0.5%.

with surface-sensitive techniques. Since the N-doped diamond is insulating at room temperature, the charging effects were compensated by illuminating the substrate by an argon ion laser for the XPS measurements.

Changes in band bending with different annealing temperatures successively removing hydrogen from the surface are illustrated by the XP normal emission spectra of the C 1s core level in Fig. 4 (the XPS measurements were carried out at room temperature). The Gaussian fit of the C 1s core level (bulk and surface contributions) was mainly done to determine the C–C bulk position. For the N-doped (100)-(2 × 1):H surface it is situated at 286.7 eV binding energy and shifts successively towards lower binding energies (285.4 eV for the (100)-(2 × 1) surface). The positions and the shifts are in agreement with the measurements of Smentkowski et al. [27]. For the (100)-(2 × 1) surface, the π-bond dimers are responsible for the formation of occupied and unoccupied surface states [19]. Nitrogen acts as a donor and, therefore, the electrons of the high-lying bulk donor levels populate the lower-lying unoccupied surface states. Owing to this charge transfer, E_F drops (therefore upward band bending) and the surface bands fill until thermodynamic equilibrium is achieved.

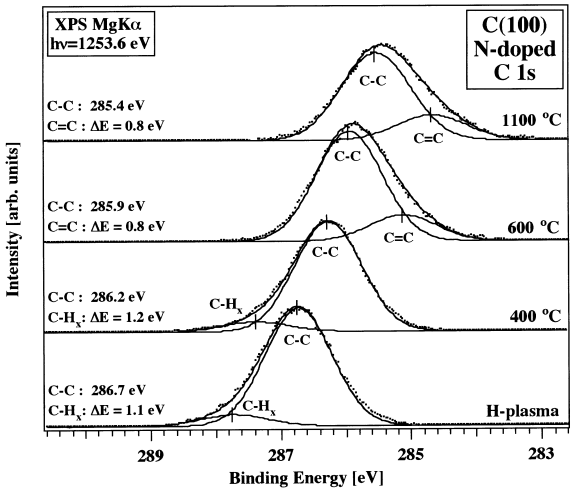

Fig. 4. XP normal emission spectra (Mg Kα, $h\nu = 1253.6$ eV) of the C 1s core level obtained after heating the hydrogen-terminated N-doped diamond (100) surface to temperatures up to 1100°C resulting in a hydrogen-free surface.

Because the density of surface states N_D ($\approx 10^{15}$ cm^{-2}) is high, E_F of the hydrogen-free (100)-(2 × 1) surface is pinned independently of the bulk dopant density [37]. The shifts of the bulk C 1s core levels for the differently terminated N-doped (100) surfaces lead to an increasing upward band bending and therefore to a change in surface Fermi-level pinning. A detailed spectrum of the C 1s core level shows different shoulders, which change intensity during annealing [18]. The C 1s core level of the (100)-(2 × 1):H surface has a shoulder at higher binding energies while the (100)-(2 × 1) surface presents a shoulder at lower binding energies. The shoulder at higher binding energies can be explained by the C–H_x ($1 < x \leq 3$) bonds whereas the shoulder at lower binding energies is due to the H-free π-bonded dimers [13].

The relative position of the VBM with respect to E_F obtained after annealing the (100)-(2 × 1):H surface to temperatures up to 1100°C is shown in the He II normal emission spectra in Fig. 5. The insulating behavior of the N-doped diamond at room temperature and therefore charging in UPS was eliminated by doing the UPS measurements at a substrate temperature of 400°C, where the

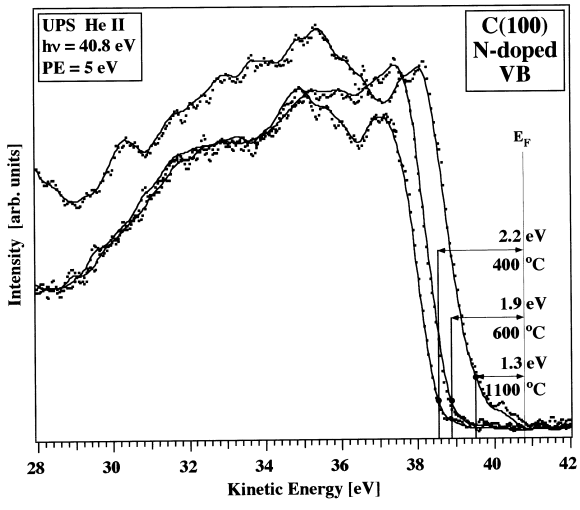

Fig. 5. He II ($h\nu = 40.8$ eV) normal emission spectra of the valence band after heating the hydrogen-saturated N-doped diamond (100) surface to temperatures up to 1100°C. The numbers given in the graph present the respective energy distances between the Fermi level E_F and the valence band maximum. The spectra has been measured with a pass energy PE = 5 eV.

crystal is conductive. The Fermi level E_F (located at 40.8 eV kinetic energy) was determined from the He II spectra of the molybdenum sample holder. We assume the VBM at the position with extrapolation of the valence band to zero intensity (Fig. 5). The diamond (100)-(2 × 1):H surface is known to have no surface states near E_F [19,32], states near the Γ-point of the bulk BZ are probed and therefore the determination of the VBM for this surface termination is possible. For the (100)-(2 × 1):H surface annealed to 400°C, the VBM is determined to be 2.2 eV below E_F what corresponds to an upward band bending of 1.7 eV (E_F lies at 1.6 eV below the CBM in the bulk [36] and a band gap value of 5.5 eV) for the N-doped surface. The UP spectrum of the (100)-(2 × 1) surface shows no major differences (no sharp surface states) which allows us to determine the VBM at 1.3 eV below E_F corresponding to an upward band bending of 2.6 eV. The annealing process did not induce major changes in the He II spectra except for the relative position of the VBM with respect to E_F. The (100)-(2 × 1) surface (annealed to 1100°C) shows a small contribution centered at a kinetic energy of 40.1 eV near E_F, which might be a surface state. Further experiments (such as ARUPS measurements) have to be done.

An interesting question is whether the hydrogen-terminated N-doped diamond (100) surface shows NEA like the hydrogen-terminated B-doped diamond (100)-(2 × 1) surface [18,19]. The NEA behavior for the B-doped diamond (100)-(2 × 1):H surface is normally detected by a peak of extremely high intensity at low kinetic energies in the He I spectrum (Fig. 1, notice the different intensity scales) and it is at the position of the CBM located above E_{vac}. In the case of PEA the electrons are emitted into vacuum down to the vacuum level (located above the CBM). He I normal emission spectra are presented in Fig. 6 for the N-doped, 400–1100°C annealed (100)-(2 × 1) surfaces. The relative position of the CBM with respect to E_F is chosen by the cutoff of the NEA peak with extrapolation to zero intensity. The spectra cutoff of the 400°C annealed surface is situated at 3.1 eV. In fact deducing the energy distance $E_F - CBM = 3.1$ eV from the band gap (i.e. 5.5 eV), we obtain 2.4 eV for the energy distance

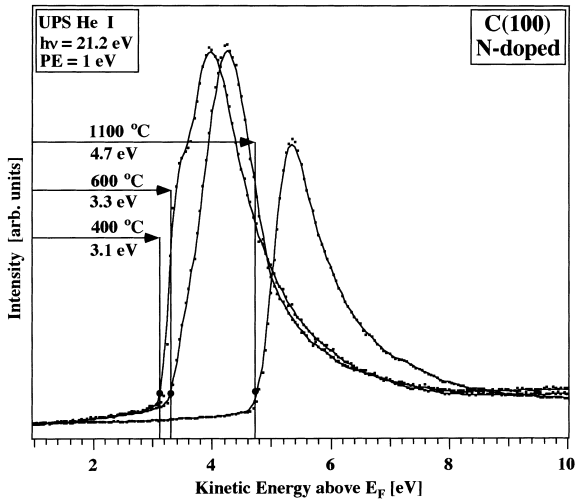

Fig. 6. Low kinetic energy part of the He I ($h\nu = 21.2$ eV) normal emission spectra of the valence band after heating the hydrogen-terminated N-doped diamond (100) surface to temperatures up to 1100°C. The energy scale is corrected for a bias of 1.5 V applied to the sample to overcome the work function of the analyzer. The numbers given in the graph present the cutoff energy position with extrapolation to zero intensity. The spectra has been measured with a pass energy PE = 1 eV.

VBM − E_F which is greater than that determined with the He II spectra. The spectrum cutoff increases to 3.3 eV while the intensity do not change. For the 1100°C annealed surface, the spectrum cutoff further increases to 4.7 eV while the intensity has decreased. The 400 and 600°C annealed surfaces present weak shoulders at the low kinetic energy part of the spectra.

3.3. Boron-doped diamond (100) surface

The B-doped, type IIb diamond (100) surface cleaned by a hydrogen plasma [20,29] is stable in air and it presents no surface contamination as shown by the XP normal emission overview spectrum (Mg Kα, $h\nu = 1253.6$ eV) in Fig. 3. Atomic force microscope images show a very smooth surface with a mean roughness lower than 5 Å (RMS) [29] while the LEED pattern shows a clear (2 × 1) reconstruction on the as introduced surface [18,21].

The change in band bending after annealing the (100)-(2 × 1):H surface up to 1100°C is illustrated

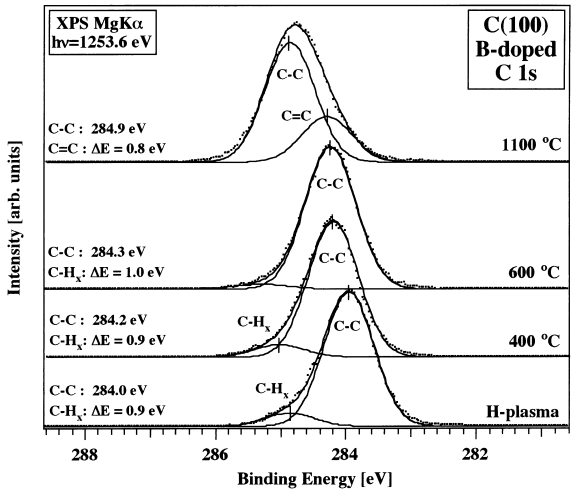

Fig. 7. XPS normal emission spectra (Mg Kα, $h\nu = 1253.6$ eV) of the C 1s core level obtained after heating the hydrogen-terminated B-doped diamond (100) surface to temperatures up to 1100°C resulting in a hydrogen-free surface.

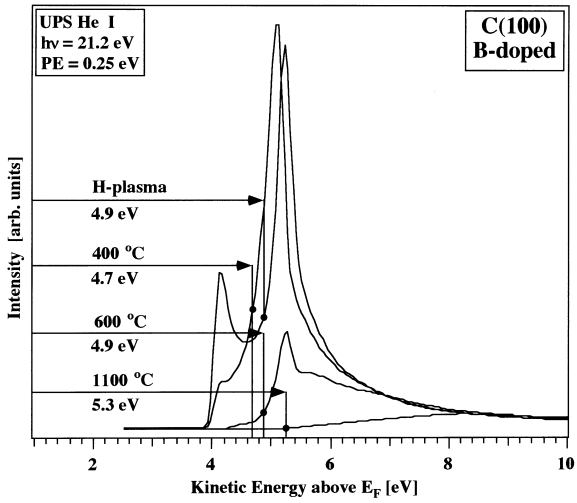

Fig. 8. Low kinetic energy part of the He I ($h\nu = 21.2$ eV) normal emission photoelectron spectra of the valence band after heating the hydrogen-terminated B-doped diamond (100) surface to temperatures up to 1100°C. The energy scale is corrected for a bias of 1.5 V applied to the sample to overcome the work function of the analyzer. The numbers given in the graph present the cutoff energy position with extrapolation to zero intensity. The spectra were measured with a pass energy PE = 0.25 eV.

by the XP normal emission spectra of the C 1s core level as shown in Fig. 7. The bulk C 1s core level for the (100)-(2 × 1):H surface is situated at 284.0 eV binding energy and shifts successively towards higher energies (284.9 eV for the (100)-(2 × 1) surface). The shifting of the C 1s core level indicates an increasing downward band bending and is in perfect agreement with earlier measurements done on the same surface [18]. The downward band bending is because boron acts as an acceptor. The different shoulders of the C 1s core level which change intensity during annealing have been explained for the N-doped diamond surface and discussed elsewhere [13,18].

The relative position of the VBM with respect to E_F measured by He II has been presented in earlier experiments [18,19].

He I normal emission spectra are presented in Fig. 8 for the B-doped (100)-(2 × 1):H surface after annealing it up to 1100°C in order to clearly observe the NEA and PEA behavior. The (100)-(2 × 1):H surface shows NEA behavior, in agreement with calculations [26] and experimentally observed by the high intensity peak situated at 4.9 eV kinetic energy (by extrapolation to zero intensity). A peak at a lower kinetic energy than the NEA peak is observed and characterizes the spectrum cutoff. The photoelectron emission below the CBM up to the vacuum level will be discussed in Section 4. After annealing up to 400°C the cutoff position of the NEA peak has shifted to 4.7 eV while the spectra cutoff is still situated at 3.9 eV. After annealing up to 600°C the NEA peak shifts back to 4.9 eV. The shifting reverses because the NEA peak vanishes successively on going up to 1100°C [19]. The (100)-(2 × 1) surface has its cutoff situated at 5.3 eV, therefore showing a PEA (the cutoff energy position is greater than the energy distance $E_F - CBM$) as predicted by calculations [23,26].

4. Discussion

The previously presented UPS and XPS results allow us to draw the energy band diagrams for the N- and B-doped diamond (100) surfaces presented in Fig. 9. In order to understand these band

diagrams better, we discuss in detail the N- and B-doped diamond (100) surfaces for the case of 400°C annealing. For the N-doped diamond surface, deducing $VBM - E_F = 2.2$ eV (determined from Fig. 5) from the band gap (i.e. 5.5 eV), we obtain 3.3 eV for the energy distance $E_F - CBM$ and 1.7 eV for the upward band bending. The measured energy distance between E_{vac} and E_F is 3.1 eV (determined from Fig. 6) resulting in a NEA of -0.2 eV estimating an error of 0.1 eV. For the B-doped diamond surface, deducing $E_F - CBM = 4.7$ eV (determined from Fig. 8) from the band-gap (5.5 eV), we obtain 0.8 eV for the energy distance $VBM - E_F$ and 0.5 eV downward band bending. Deducing the energy distance between E_{vac} and E_F characterized by the spectra cutoff at 3.9 eV (determined from Fig. 8) from the distance $E_F - CBM = 4.7$ eV results in a NEA of -0.8 eV estimating an error of 0.1 eV. Therefore the He I normal emission spectra (position of the cutoff with extrapolation to zero intensity) allow us to fix the distance between E_F and the CBM or between E_F and E_{vac}, respectively. The increasing band bending of the two differently doped diamond surfaces was determined by the shifts of the C 1s core levels (Figs. 4 and 7) while the energy distances $E_F - VBM$ were determined by the He II normal emission spectra (Fig. 5). Both the B- and N-doped (100)-(2×1):H surfaces show NEA by determining the energy positions of the UP spectra by the cutoff with extrapolation to zero intensity. A different energy position determination would change the interpretation and especially the electron affinity. The fact that we determine NEA values for the hydrogen-terminated B- and N-doped diamond (100) surfaces suggests that we measure electron emission below the CBM. By secondary electron emission spectroscopy, Yater et al. [38] also observed this low kinetic energy shoulder but for the cesiated diamond (100) surface. They suggested that for a high NEA value, low kinetic energy electrons at the surface, which populate energy levels below the CBM (unoccupied surface states) can still be emitted into the vacuum [38]. Therefore, the low kinetic energy shoulders or peaks of the spectra, respectively, characterize the emission from energy levels below the CBM up to the vacuum level E_{vac} (supposing E_{vac} at the cutoff position of the spectra) and permit therefore to determine an upper limit at the NEA value. If E_{vac} is at an even lower position then the NEA value is higher. Using photoelectron yield spectroscopy, Ristein et al. [39,40] also measured photoelectrons below the CBM. They accorded the electrons to emission from defects.

The work function ϕ of the B-doped diamond is slightly higher than that for the N-doped diamond. Similar results have been found for p- and n-type silicon surfaces [30,41,42]. Cardona and Ley [30] state that the work function ϕ of a semiconductor is defined with respect to its Fermi level, which can be altered by doping or by surface reconstruction. The different work function values result from the fact that the Fermi level E_F at the surface is not pinned exactly in the middle of the band gap (E_F of the p-type surface is nearer to the VBM and E_F of the n-type surface is nearer to the CBM) [30,41,42]. The differently pinned Fermi levels for the hydrogen-terminated N- and B-doped diamond surfaces is due to the fact that hydrogen removes the π-type surface states inducing a flattening of the bands at the surface. The (100)-(2×1):H surfaces have a work function approximately 1.5 eV lower than that for the (100)-(2×1) surfaces. Similarly to alkalis on metal surfaces, H-termination with C–H bonds at the surface results in a surface dipole layer, decreasing ϕ of the diamond (100) surface by approximately 1.5 eV. It is then a logical consequence that we observe a slightly different NEA value for the N- and B-doped diamond (100) surfaces. The quantity which changes similarly for the two different terminated N- and B-doped diamond (100) surfaces is the work function while the energy distance $E_F - CBM$ and the band bending change differently.

The hydrogen-terminated N and B-doped diamond (100) surfaces show NEA because of the wide band gap (i.e. 5.5 eV) and the reduced work function (due to hydrogen termination). In addition, the B-doped diamond (100)-(2×1):H surface shows a small downward band bending and therefore the electrons can easily escape to the vacuum by forming a high intensity peak observed experi-

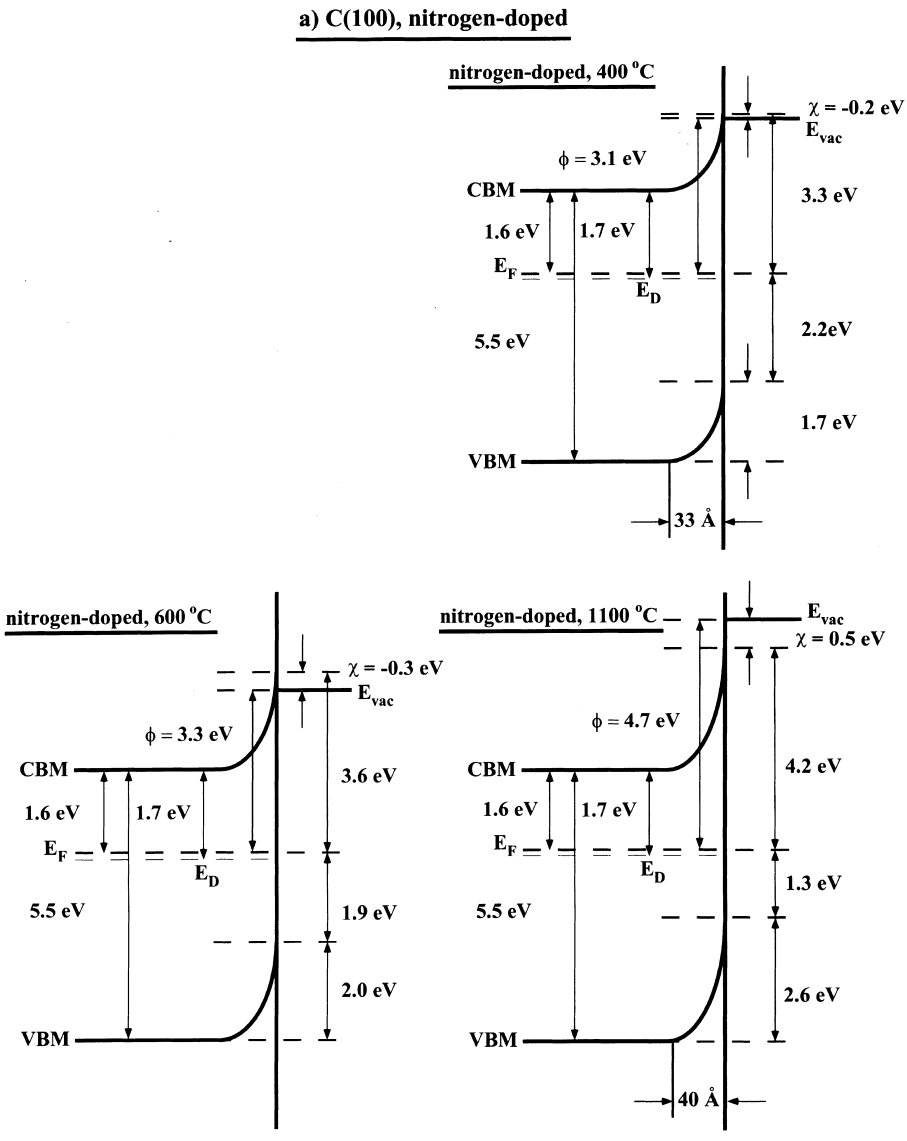

Fig. 9. Energy band diagrams of the (a) N- and (b) B-doped diamond (100) surfaces after heating the (100)-(2 × 1):H surfaces to temperatures up to 1100°C resulting in (100)-(2 × 1) surfaces. The values are estimated to lie within an error value of 0.1 eV.

mentally by UPS. In contrast to the B-doped (100)-(2 × 1):H surface, UPS measurements on the N-doped (100)-(2 × 1):H surface do not reveal a high intensity NEA peak due to the strong upward band bending. The electrons have to overcome the barrier of upward band bending at the surface (therefore not forming an NEA peak). A similar effect was observed by Spicer [43], who showed by photoemission studies on alkali–antimony compounds that the most efficient emitters are those with p-type behavior. Like the downward and upward band banding of B- and N-doped diamond, respectively, the bands of n-type alkali–antimony compounds have the tendency to turn upward at the surface reflected by an increasing of the electron affinity barrier [43].

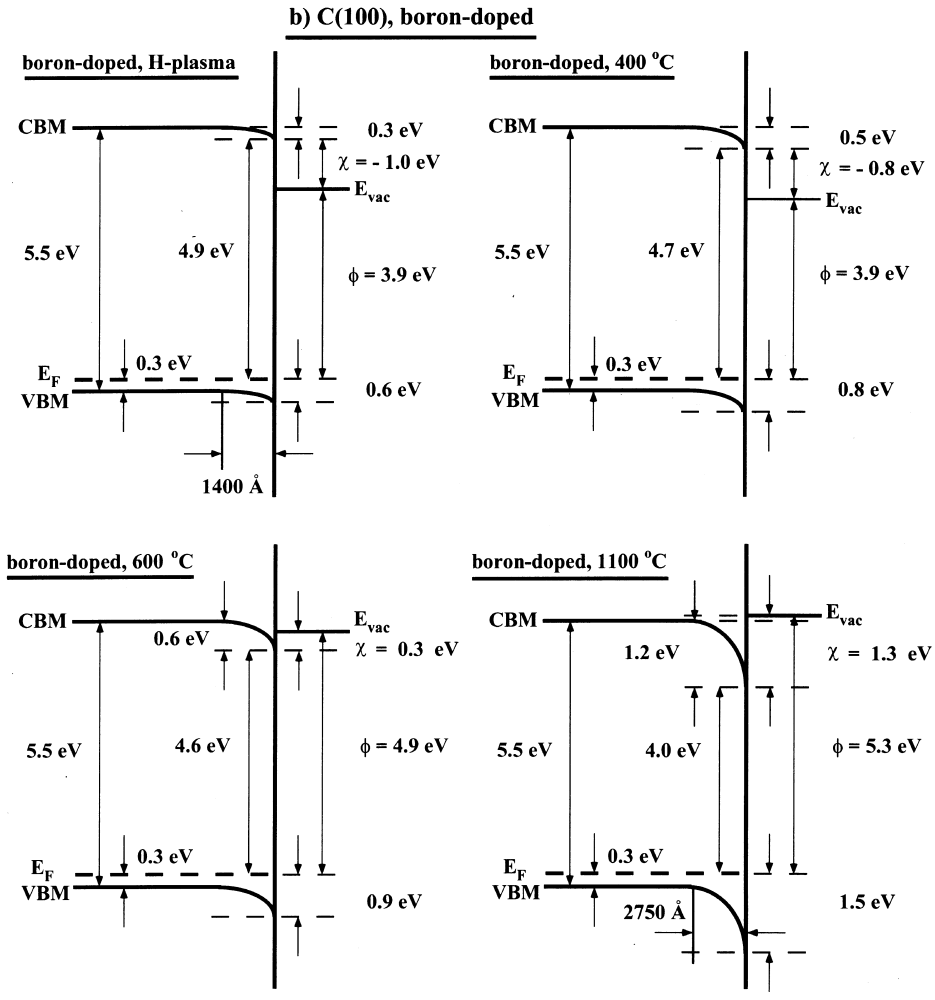

Fig. 9. (*Continued*).

5. Conclusion

The N-doped diamond (100) surface with hydrogen termination has been investigated by means of XPS and UPS for different annealing temperatures. Photoelectron emission data from the B- and the N-doped diamond (100) surfaces permit the energy band diagrams for the differently terminated (100) surfaces to be drawn. The Fermi level E_F is situated at 1.6 eV below the CBM for the N-doped diamond (100) surface, while for the B-doped diamond (100) surface E_F is situated at 0.3 eV above the VBM. Annealing the crystals to temperatures of up to 1100°C leads, for the N-doped diamond (100) surface, to an increasing upward band bending due to the donor ability of nitrogen, and for the B-doped diamond (100) surface to an increasing downward band bending due to the acceptor ability of boron as shown by XPS. Both (100)-(2×1):H surfaces show NEA as measured by UPS. In contrast to the B-doped diamond (100) surface with hydrogen termination, UPS measurements on the N-doped diamond (100)-(2×1):H surface did not reveal a high intensity NEA peak. The high intensity NEA peak of B-doped diamond seems to be due to the downward band bending together with the reduced work function because of hydrogen termination. The

work function increases for subsequent hydrogen desorption at higher annealing temperatures with associated loss of NEA. For the N-doped diamond (100) surface the work function behaves similarly but the observation of a NEA peak is absent because of the surface barrier formed by the high upward band bending.

Acknowledgements

We thank L. Ley, and J. Ristein for the fruitful discussions, F. Bourqui, Ch. Neururer, E. Mooser, and O. Raetzo for the skilful technical assistance. The authors gratefully acknowledge financial support by the Swiss Priority Program Materials and the Swiss National Science Foundation. Part of this work was carried out under the auspices of the trinational "D–A–CH" cooperation of Germany, Austria, and Switzerland on the "Synthesis of Superhard Materials".

References

[1] J.E. Field, The Properties of Natural and Synthetic Diamond, Academic Press, London, 1992.
[2] K.E. Spear, J.P. Dismukes, Synthetic Diamond: Emerging CVD Science and Technology, Wiley, New York, 1994.
[3] L.S. Pan, D.R. Kania, Diamond: Electronic Properties and Applications, Kluwer, Boston, MA, 1995.
[4] R.G. Farrer, Solid State Commun. 7 (1969) 685.
[5] S.A. Kajihara, A. Antonelli, J. Bernholc, Phys. Rev. Lett. 66 (1991) 2010.
[6] R. Samlenski, C. Haug, R. Brenn, C. Wild, R. Locher, P. Koidl, Appl. Phys. Lett. 67 (1995) 2798.
[7] R. Locher, C. Wild, N. Herres, D. Behr, P. Koidl, Appl. Phys. Lett. 65 (1994) 34.
[8] K. Okano, S. Koizumi, S. Ravi, P. Silva, G.A.J. Amaratunga, Nature 381 (1996) 140.
[9] M.W. Geis, J.C. Twichell, N.N. Efremow, K. Krohn, T.M. Lyszczarz, Appl. Phys. Lett. 68 (1996) 2294.
[10] M.W. Geis, J.C. Twichell, J. Macaulay, K. Okano, Appl. Phys. Lett. 67 (1995) 1328.
[11] M.W. Geis, J.C. Twichell, T.M. Lyszczarz, J. Vac. Sci. Technol. B 14 (1996) 2060.
[12] P. Lerner, P.H. Cutler, N.M. Miskovsky, J. Vac. Sci. Technol. B 15 (1997) 337.
[13] B.B. Pate, Surf. Sci. 165 (1986) 83.
[14] T.E. Derry, L. Smit, J.F. van der Veen, Surf. Sci. 167 (1986) 502.
[15] A.V. Hamza, G.D. Kubiak, R.H. Stulen, Surf. Sci. 237 (1990) 35.
[16] B.D. Thoms, J.E. Butler, Surf. Sci. 328 (1995) 291.
[17] F.J. Himpsel, J.F. van der Veen, D.E. Eastman, Phys. Rev. B 22 (1980) 1967.
[18] L. Diederich, O.M. Küttel, E. Maillard-Schaller, L. Schlapbach, Surf. Sci. 349 (1996) 176.
[19] L. Diederich, P. Aebi, O.M. Küttel, E. Maillard-Schaller, R. Fasel, L. Schlapbach, Surf. Sci. 393 (1997) L77.
[20] O.M. Küttel, R.G. Agostino, R. Fasel, J. Osterwalder, L. Schlapbach, Surf. Sci. 312 (1994) 131.
[21] O.M. Küttel, L. Diederich, E. Schaller, O. Carnal, L. Schlapbach, Surf. Sci. 337 (1995) L812.
[22] C. Nützenadel, O.M. Küttel, L. Diederich, E. Maillard-Schaller, O. Gröning, L. Schlapbach, Surf. Sci. 369 (1996) L111.
[23] J. Furthmüller, J. Hafner, G. Kresse, Phys. Rev. B 53 (1996) 7334.
[24] D.R. Alfonso, D.A. Drabold, S.E. Ulloa, Phys. Rev. B 51 (1995) 14669.
[25] Th. Frauenheim, U. Stephan, P. Blaudeck, D. Porezag, H.-G. Busmann, W. Zimmermann-Edling, S. Lauer, Phys. Rev. B 48 (1993) 18189.
[26] Z. Zhang, M. Wensell, J. Bernholc, Phys. Rev. B 51 (1995) 5291.
[27] V.S. Smentkowski, H. Jänsch, M.A. Henderson, J.T. Yates, Surf. Sci. 330 (1995) 207.
[28] W.E. Pickett, Phys. Rev. Lett. 73 (1994) 1664.
[29] L. Diederich, O.M. Küttel, P. Aebi, L. Schlapbach, Surf. Sci., in press.
[30] M. Cardona, L. Ley, Photoemission in Solids I, Springer, Berlin, 1978.
[31] G.V. Hansson, R.I.G. Uhrberg, Surf. Sci. Rep. 9 (1988) 225.
[32] R. Graupner, M. Hollering, A. Ziegler, J. Ristein, L. Ley, A. Stampfl, Phys. Rev. B 55 (1997) 10841.
[33] E.C. Lightlowlers, A.T. Collins, J. Phys. D 9 (1976) 951.
[34] A.T. Collins, A.W.S. Williams, J. Phys. C 4 (1971) 1789.
[35] C. Bandis, B.B. Pate, Phys. Rev. B 52 (1995) 12056.
[36] L. Diederich, J. Ristein, O.M. Küttel, L. Ley, L. Schlapbach, in preparation.
[37] A. Zangwill, Physics at Surfaces, Cambridge University Press, Cambridge, 1988.
[38] J. Yater, A. Shih, R. Abrams, Phys. Rev. B 56 (1997) R4410.
[39] J. Ristein, W. Stein, L. Ley, Phys. Rev. Lett. 78 (1997) 1803.
[40] J. Ristein, W. Stein, L. Ley, Diamond Relat. Mater. 7 (1998) 626.
[41] L.F. Wagner, W.E. Spicer, Phys. Rev. B 9 (1974) 1512.
[42] L. Ley, J. Ristein, J. Schäfer, S. Miyazaki, J. Vac. Sci. Technol. B 14 (1996) 3008.
[43] W.E. Spicer, Phys. Rev. 112 (1958) 114.